Electronic Supplementary Material (ESI) for Journal of Materials Chemistry C.

Supplementary Information for "Promising photovoltaic and solid-state-lighting materials: two-dimensional Ruddlesden-Popper type lead-free halide double perovskites $Cs_{n+1}In_{n/2}Sb_{n/2}I_{3n+1}$ (n=3) and $Cs_{n+1}In_{n/2}Sb_{n/2}Cl_{3n+1}/Cs_{m+1}Cu_{m/2}Bi_{m/2}Cl_{3m+1}$ (n=3, m=1)"

Meng Wu,[a] Jun-jie Shi,[*,a] Min Zhang,[b] Yu-lang Cen,[a] Wen-hui Guo[a] and Yao-hui Zhu[c]

[a]*State Key Laboratory for Artificial Microstructures and Mesoscopic Physics, School of Physics, Peking University, Beijing 100871, China*
[b]*College of Physics and Electronic Information, Inner Mongolia Normal University, Hohhot 010022, China*
[c]*Physics Department, Beijing Technology and Business University, Beijing 100048, China*

*E-mail: jjshi@pku.edu.cn

Table S1 Values of the parameter *CUT* (in atomic units) and *l* together with the detailed half-ionized orbitals for M^+, M^{3+} and X^- in our GGA-1/2 calculations are listed. Our *CUT* values for X^- are slightly smaller than those of ref. a-c (3.12, 3.34 and 3.76 for Cl^-, Br^- and I^-). This is because the anion *CUT* value usually has a small dependence on the chemical environment, as pointed out by Ferreira *et al.*[d]

Atom	*CUT*	*l*	Half-ionized orbital	Atom	*CUT*	*l*	Half-ionized orbital
In^+	2.6	100	d	Sb^{3+}	2.8	90	d
Cu^+	2.8	100	d	Cl^-	2.9	100	p
Ag^+	3.1	100	d	Br^-	3.1	100	p
Au^+	3.0	100	d	I^-	3.4	100	p
Bi^{3+}	2.7	90	d				

[a] J. Jiang, C. K. Onwudinanti, R. A. Hatton, P. A. Bobbert and S. Tao, *J. Phys. Chem. C,* 2018, **122**, 17660.

[b] K. P. Marshall, S. Tao, M. Walker, D. S. Cook, J. Lloyd-Hughes, S. Varagnolo, A. Wijesekara, D. Walker, R. I. Walton and R. A. Hatton, *Mater. Chem. Front.,* 2018, **2**, 1515.

[c] S. X. Tao, X. Cao and P. A. Bobbert, *Sci. Rep.*, 2017, **7**, 14386.

[d] L. G. Ferreira, M. Marques and L. K. Teles, *Phys. Rev. B: Condens. Matter Mater. Phys.*, 2008, **78**, 125116.

Table S2 The dependence of the GGA-1/2 bandgap on the half-ionized orbitals of metal atoms in $Cs_2In_{1/2}Sb_{1/2}I_4$ and $Cs_2Cu_{1/2}Bi_{1/2}Cl_4$, in which the half ionization of the *p*-orbital in I and Cl atoms is included. Compared with the accurate GW bandgap, we can easily find that the correction of *d* orbital for both M^+ and M^{3+} is necessary

Material	Half-ionized orbital	Bandgap (eV)
$Cs_2In_{1/2}Sb_{1/2}I_4$	In: × Sb: ×	0.58
	In: p Sb: ×	0.62
	In: d Sb: ×	1.23
	In: d Sb: p	1.40
	In: d Sb: d	1.55, 1.55(GW)
$Cs_2Cu_{1/2}Bi_{1/2}Cl_4$	Cu: × Bi: ×	2.34
	Cu: p Bi: ×	2.80
	Cu: d Bi: ×	3.58
	Cu: d Bi: p	3.64
	Cu: d Bi: d	3.82, 3.82(GW)

Table S3 Fully optimized lattice parameter *a* (in unit of Å) in lead-free *n*=1 halide Cs_2M+ 1/2M3+ 1/2X 4 double perovskites. Some previous experimental results in bulk phase are also given

<table>
<tr><th>Cs_2M+ 1/2M3+ 1/2</th><th>X</th><th colspan="2">*a*</th><th>Cs_2M+ 1/2M3+ 1/2</th><th>X</th><th>*a*</th></tr>
<tr><td rowspan="3">$Cs_2In_{1/2}Bi_{1/2}$</td><td>Cl</td><td colspan="2">11.22</td><td rowspan="3">$Cs_2Cu_{1/2}Bi_{1/2}$</td><td>Cl</td><td>11.00</td></tr>
<tr><td>Br</td><td colspan="2">11.73</td><td>Br</td><td>11.50</td></tr>
<tr><td>I</td><td colspan="2">12.32</td><td>I</td><td>12.36</td></tr>
<tr><td rowspan="3">$Cs_2In_{1/2}Sb_{1/2}$</td><td>Cl</td><td colspan="2">11.10</td><td rowspan="3">$Cs_2Cu_{1/2}Sb_{1/2}$</td><td>Cl</td><td>10.89</td></tr>
<tr><td>Br</td><td colspan="2">11.60</td><td>Br</td><td>11.37</td></tr>
<tr><td>I</td><td colspan="2">12.28</td><td>I</td><td>12.34</td></tr>
<tr><td rowspan="7">$Cs_2Ag_{1/2}Bi_{1/2}$</td><td rowspan="3">Cl</td><td>n=1 2D</td><td>10.98</td><td rowspan="7">$Cs_2Au_{1/2}Bi_{1/2}$</td><td rowspan="3">Cl</td><td rowspan="3">11.51</td></tr>
<tr><td rowspan="2">bulk $Cs_2AgBiCl_6$</td><td>10.78[(exp)a]</td></tr>
<tr><td>10.85</td></tr>
<tr><td rowspan="3">Br</td><td>n=1 2D</td><td>11.53</td><td rowspan="3">Br</td><td rowspan="3">11.95</td></tr>
<tr><td rowspan="2">bulk $Cs_2AgBiBr_6$</td><td>11.27[(exp)b]</td></tr>
<tr><td>11.30</td></tr>
<tr><td>I</td><td colspan="2">12.36</td><td>I</td><td>12.64</td></tr>
<tr><td rowspan="3">$Cs_2Ag_{1/2}Sb_{1/2}$</td><td>Cl</td><td colspan="2">10.87</td><td rowspan="3">$Cs_2Au_{1/2}Sb_{1/2}$</td><td>Cl</td><td>11.39</td></tr>
<tr><td>Br</td><td colspan="2">11.41</td><td>Br</td><td>11.82</td></tr>
<tr><td>I</td><td colspan="2">12.24</td><td>I</td><td>12.42</td></tr>
</table>

[a] E. T. Mcclure, M. R. Ball, W. Windl and P. M. Woodward, *Chem. Mater.*, 2016, **28**, 1348.
[b]A. H. Slavney, T. Hu, A. M. Lindenberg and H. I. Karunadasa, *J. Am. Chem. Soc.*, 2016, **138**, 2138.

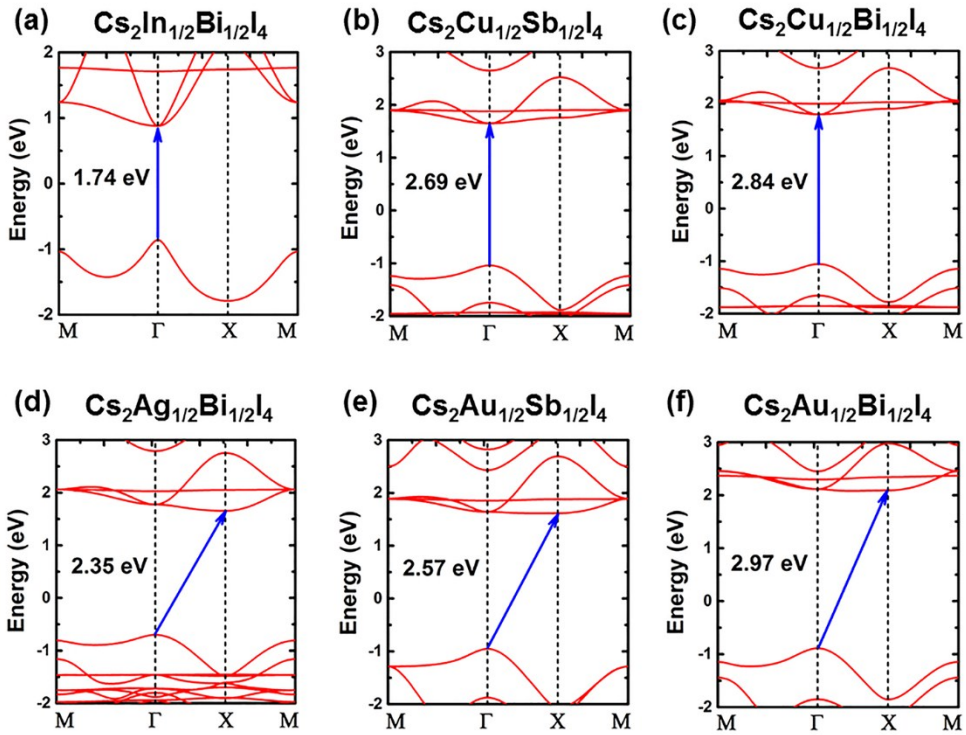

Figure S1 Energy band structures of *n*=1 lead-free halide double perovskites with direct bandgap (a) $Cs_2In_{1/2}Bi_{1/2}I_4$, (b) $Cs_2Cu_{1/2}Sb_{1/2}I_4$ and (c) $Cs_2Cu_{1/2}Bi_{1/2}I_4$, and indirect bandgap (d) $Cs_2Ag_{1/2}Bi_{1/2}I_4$, (e) $Cs_2Au_{1/2}Sb_{1/2}I_4$ and (f) $Cs_2Au_{1/2}Bi_{1/2}I_4$. Here, the band structures are derived from the GGA-PBE calculations, in which the underestimated bandgaps are modified according to GGA-1/2 calculations.

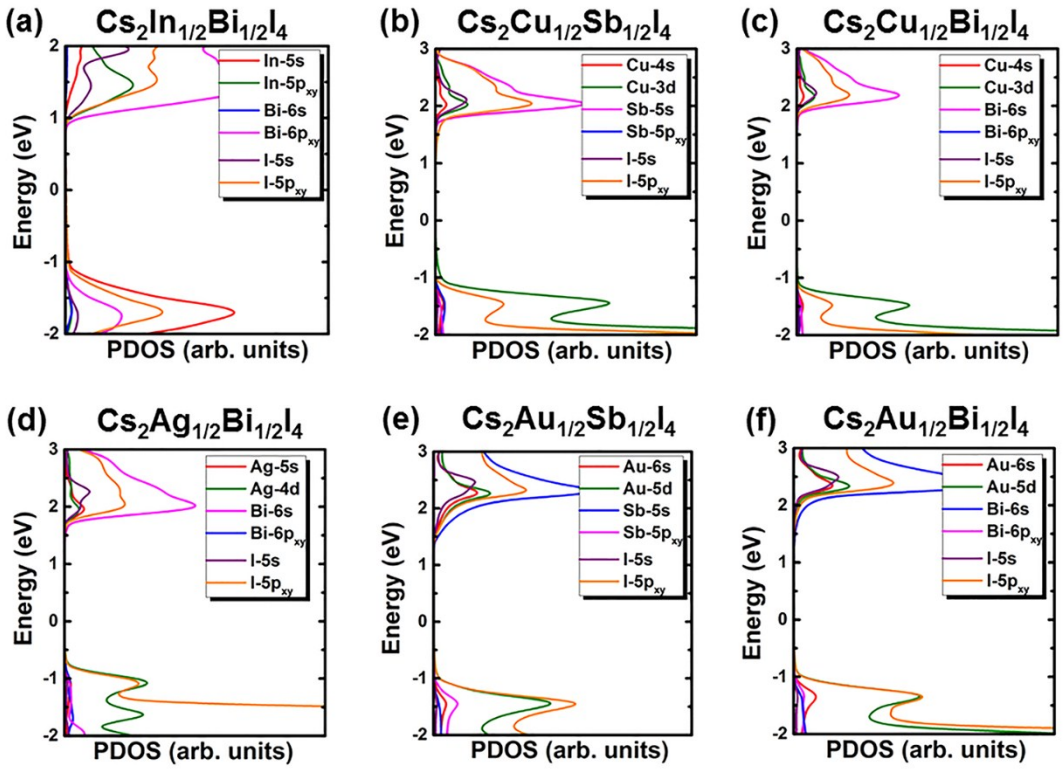

Figure S2 PDOSs of *n*=1 lead-free halide double perovskites with direct bandgap (a) $Cs_2In_{1/2}Bi_{1/2}I_4$, (b) $Cs_2Cu_{1/2}Sb_{1/2}I_4$ and (c) $Cs_2Cu_{1/2}Bi_{1/2}I_4$, and indirect bandgap (d) $Cs_2Ag_{1/2}Bi_{1/2}I_4$, (e) $Cs_2Au_{1/2}Sb_{1/2}I_4$ and (f) $Cs_2Au_{1/2}Bi_{1/2}I_4$.

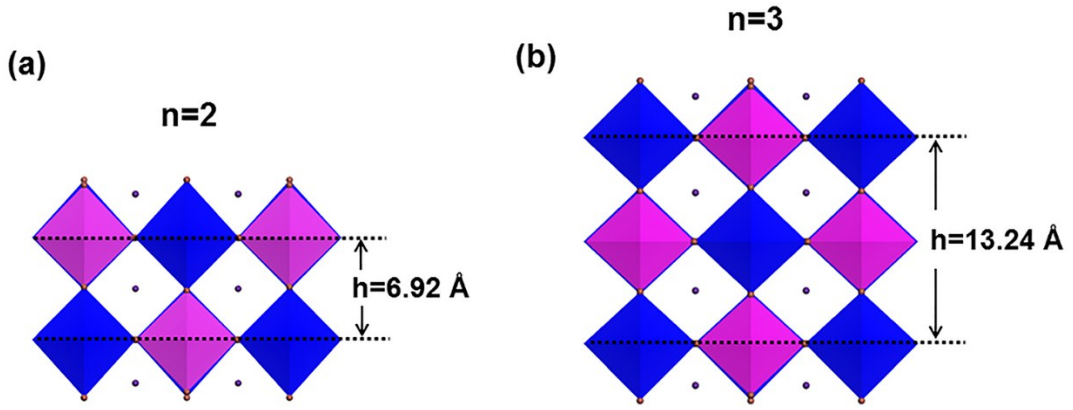

Figure S3 The 2D double perovskite crystal structures of (a) n=2 Cs_3InSbI_7 and (b) n=3 $Cs_4In_{3/2}Sb_{3/2}I_{10}$ with the vertical distance of h=6.92 and 13.24 Å, respectively. Here, the stacking order of layered double perovskites, composed by the alternative M^+X (pink) and $M^{3+}X$ (blue) octahedrons, is similar to their bulk counterparts.

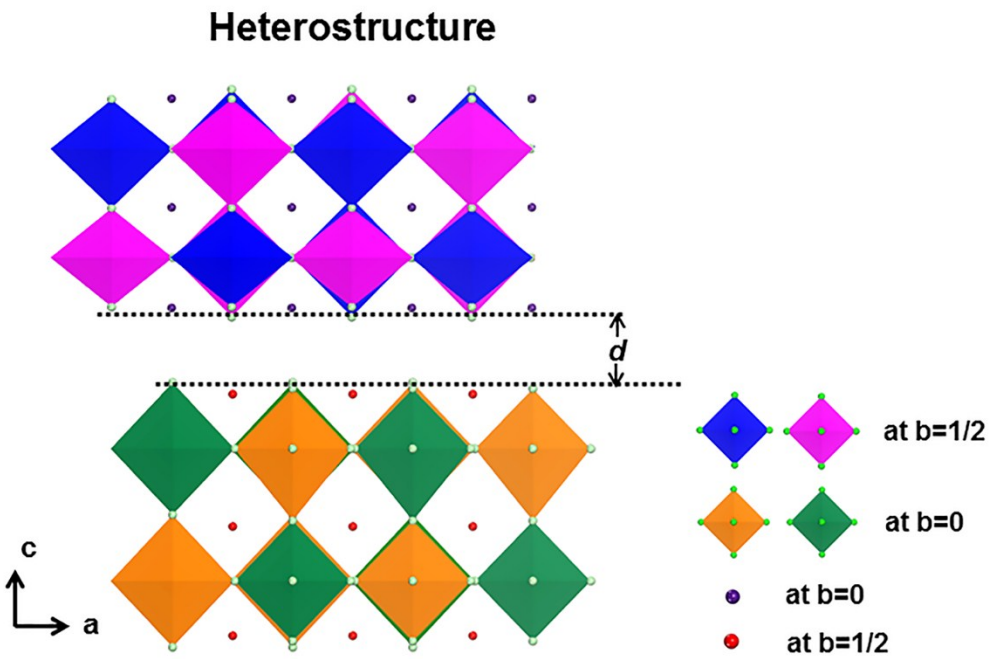

Figure S4 Schematic illustration of the crystal structure of 2D lead-free halide double perovskite heterostructure. The different perovskite layers in the heterostructure are directly stacked together with a shift of b/2 along the b-axis just as the bulk RP-type perovskite. A suitable strain exists to match the lattice constants of different layers. The d represents the interlayer distance between two different layers in the heterostructure.

Table S4 The interlayer distance *d* (Å) and lattice mismatch of all considered 2D RP-type lead-free halide double perovskite heterostructures

Material	Layer thickness	*d*	Lattice mismatch
CsInSbCl/CsCuBiCl	*n*=1/*m*=1	5.51	0.45%
	n=2/*m*=1	5.54	0.67%
	n=1/*m*=2	5.56	0.51%
	n=2/*m*=2	5.65	0.53%
	n=3/*m*=1	5.62	0.72%
CsInBiCl/CsCuBiCl	*n*=1/*m*=1	5.58	0.98%
CsInSbCl/CsAgBiCl	*n*=1/*m*=1	5.59	0.54%
CsInBiCl/CsCuSbCl	*n*=1/*m*=1	5.57	1.47%
CsAgSbBr/CsCuSbCl	*n*=1/*m*=1	5.64	2.27%
CsAgSbBr/CsCuSbBr	*n*=1/*m*=1	5.78	0.17%
CsAgSbI/CsCuSbI	*n*=1/*m*=1	5.69	0.41%

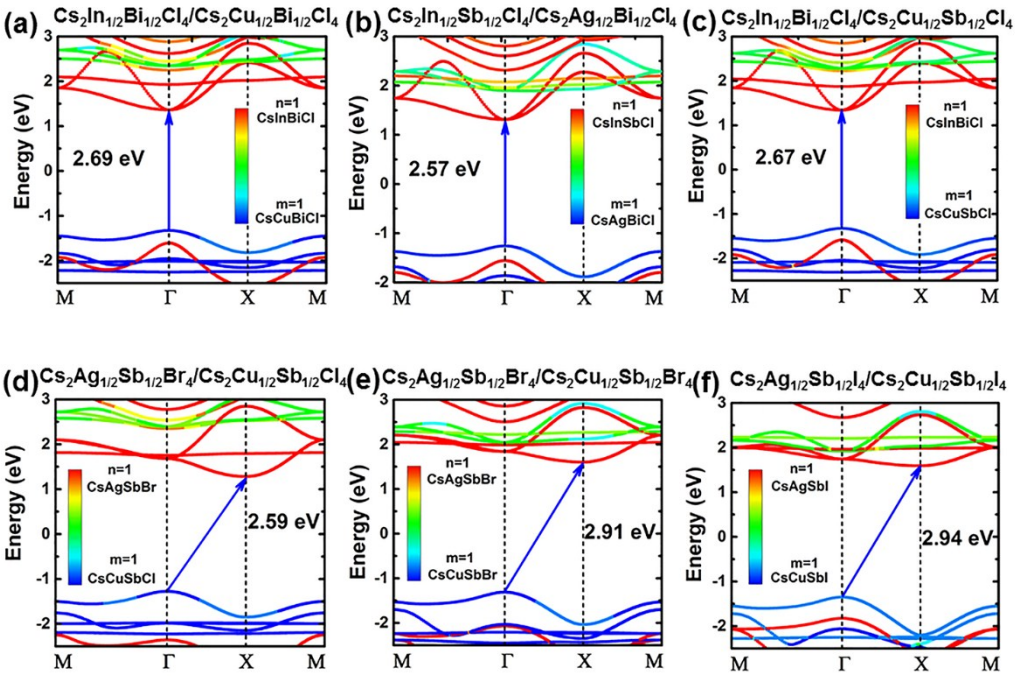

Figure S5 The weighted energy band structures of n=1/m=1 lead-free halide double perovskite heterostructures with type-II band alignment can be classified into two types, *i.e.*, direct bandgap (a) $Cs_2In_{1/2}Bi_{1/2}Cl_4/Cs_2Cu_{1/2}Bi_{1/2}Cl_4$, (b) $Cs_2In_{1/2}Sb_{1/2}Cl_4/Cs_2Ag_{1/2}Bi_{1/2}Cl_4$ and (c) $Cs_2In_{1/2}Bi_{1/2}Cl_4/Cs_2Cu_{1/2}Sb_{1/2}Cl_4$ and indirect bandgap (d) $Cs_2Ag_{1/2}Sb_{1/2}Br_4/Cs_2Cu_{1/2}Sb_{1/2}Cl_4$, (e) $Cs_2Ag_{1/2}Sb_{1/2}Br_4/Cs_2Cu_{1/2}Sb_{1/2}Br_4$ and (f) $Cs_2Ag_{1/2}Sb_{1/2}I_4/Cs_2Cu_{1/2}Sb_{1/2}I_4$. Here, the band structures are derived from the GGA-PBE calculations, in which the underestimated bandgaps are modified according to GGA-1/2 calculations.

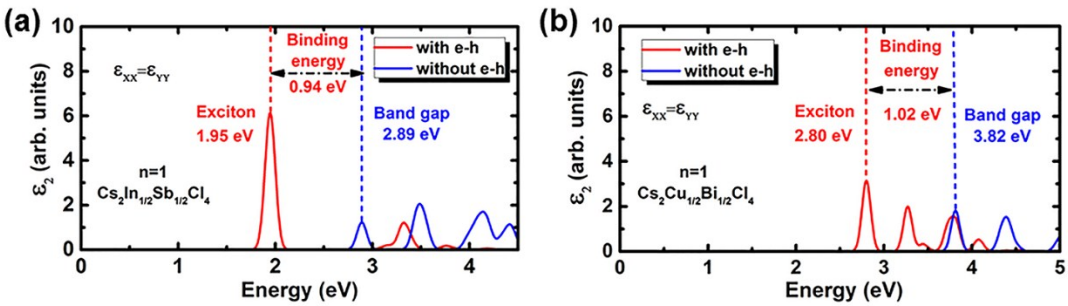

Figure S6 The calculated imaginary parts ε_2 of dielectric function for freestanding n=1 (a) $Cs_2In_{1/2}Sb_{1/2}Cl_4$ and (b) $Cs_2Cu_{1/2}Bi_{1/2}Cl_4$.

Table S5 The carrier effective mass m* (m_0) and the predicted carrier mobility μ ($cm^2V^{-1}s^{-1}$) in 2D lead-free *n*=1 halide double perovskite Cs_2M+ 1/2M3+ 1/2X 4 and their *n*=1/*m*=1 heterostructures

Material	X	m_h*	m_e*	μ_h	μ_e	Material	X	m_h*	m_e*	μ_h	μ_e
$MAPbI_3$	I	0.30	1.14	0.24		$MASnI_3$	I	0.22	1.10	0.18	
$Cs_2In_{1/2}Bi_{1/2}$	Cl	0.52	1.09	40	25	$Cs_2Cu_{1/2}Bi_{1/2}$	Cl	0.85	0.90	26	10
	Br	0.42	0.94	254	145		Br	0.81	0.88	76	58
	I	0.21	0.64	590	145		I	0.75	0.84	110	96
$Cs_2In_{1/2}Sb_{1/2}$	Cl	0.45	1.08	86	72	$Cs_2Cu_{1/2}Sb_{1/2}$	Cl	0.80	0.84	150	121
	Br	0.33	0.93	321	198		Br	0.74	0.82	230	165
	I	0.18	0.70	655	309		I	0.62	0.80	311	196
$Cs_2Ag_{1/2}Bi_{1/2}$	Cl	0.85	1.02	30	11	$Cs_2Au_{1/2}Bi_{1/2}$	Cl	0.96	1.05	40	14
	Br	0.74	0.98	101	50		Br	0.85	0.94	90	41
	I	0.66	0.93	210	121		I	0.76	0.86	160	100
$Cs_2Ag_{1/2}Sb_{1/2}$	Cl	0.83	1.06	50	30	$Cs_2Au_{1/2}Sb_{1/2}$	Cl	0.90	1.02	92	55
	Br	0.71	1.02	111	41		Br	0.81	0.89	160	117
	I	0.60	0.97	200	107		I	0.75	0.81	234	160
$Cs_2In_{1/2}Sb_{1/2}Cl_4$/ $Cs_2Cu_{1/2}Bi_{1/2}Cl_4$		0.80	0.87	70	165	$Cs_2Ag_{1/2}Sb_{1/2}Br_4$/ $Cs_2Cu_{1/2}Sb_{1/2}Cl_4$		0.76	0.72	330	90
$Cs_2In_{1/2}Bi_{1/2}Cl_4$/ $Cs_2Cu_{1/2}Bi_{1/2}Cl_4$		0.81	0.90	50	65	$Cs_2Ag_{1/2}Sb_{1/2}Br_4$/ $Cs_2Cu_{1/2}Sb_{1/2}Br_4$		0.74	0.81	395	110
$Cs_2In_{1/2}Sb_{1/2}Cl_4$/ $Cs_2Ag_{1/2}Bi_{1/2}Cl_4$		0.85	0.42	50	122	$Cs_2Ag_{1/2}Sb_{1/2}I_4$/ $Cs_2Cu_{1/2}Sb_{1/2}I_4$		0.56	0.89	598	224
$Cs_2In_{1/2}Bi_{1/2}Cl_4$/ $Cs_2Cu_{1/2}Sb_{1/2}Cl_4$		0.80	0.42	74	70						